Materials and Design 64 (2014) 246–250

Contents lists available at ScienceDirect

Materials and Design

journal homepage: www.elsevier.com/locate/matdes

Feasibility study of friction spot welding of dissimilar single-lap joint between poly(methyl methacrylate) and poly(methyl methacrylate)-SiO_2 nanocomposite

Wiebke S. Junior [a,b], Ulrich A. Handge [a,b], Jorge F. dos Santos [a,c], Volker Abetz [a,b,d,1,*], Sergio T. Amancio-Filho [a,c,e,f,2,*]

[a] Helmholtz-Zentrum Geesthacht, Centre for Materials and Coastal Research, Max-Planck-Strasse 1, D-21502 Geesthacht, Germany
[b] Institute of Polymer Research, Geesthacht, Germany
[c] Institute of Materials Research, Materials Mechanics, Solid State Joining Processes, Geesthacht, Germany
[d] University of Hamburg, Institute of Physical Chemistry, Grindelallee 117, D-20146 Hamburg, Germany
[e] Institute of Materials Research, Materials Mechanics, Advanced Polymer-Metal Hybrid Structures, Geesthacht, Germany
[f] Hamburg University of Technology, Institute of Polymer Composites, Denickestrasse 15, D-21073 Hamburg, Germany

ARTICLE INFO

Article history:
Received 15 January 2014
Accepted 23 July 2014
Available online 1 August 2014

Keywords:
Poly(methyl methacrylate)
Silica
Nanocomposite
Friction spot welding
Polymer joints

ABSTRACT

In this work, the feasibility of friction spot welding (FSpW) of a commercial poly(methyl methacrylate) (PMMA) GS grade and a PMMA 6 N/2 wt% silica (SiO_2) nanocomposite was investigated. Single-lap joints welded at rotational speeds of 1000, 2000 and 3000 rpm were produced. The analysis of the joint microstructure and material flow pattern indicated that joints could be produced using all of the tested welding conditions. However, the joint produced at 1000 rpm displayed sharp weld lines (weak links), indicating insufficient heat input, while the welds produced at 3000 rpm displayed excessive plastic deformation (bulging of the bottom plate), volumetric defects and a lack of material mixing in the welded area, associated with higher heat input. The weld produced at a rotational speed of 2000 rpm resulted in improved material mixing, which was indicated by the absence of weld lines and volumetric defects due to the more correct heat input. This welding condition was selected for further mechanical testing. Lap shear testing of PMMA GS/PMMA 6 N/2 wt% SiO_2 nanocomposite single lap joints welded at 2000 rpm resulted in an average ultimate lap shear strength of 3.9 ± 0.05 MPa. These weld strength values are equal to or better than those obtained using state-of-the-art welding techniques for PMMA materials, thereby demonstrating the potential of friction spot welding for thermoplastic nanocomposites.

1. Introduction

The development and selection of lightweight materials with tailored properties and new production technologies is a viable short- to mid-term alternative to mitigate the increasing levels of carbon dioxide (CO_2) emissions of cars and airplanes. Polymeric nanocomposites have increasingly attracted the attention of the transportation industry, due to their tailored properties, such as improved mechanical performance [1] and wear resistance [2]. Joining of polymeric nanocomposites to conventional plastics is a new subject in structural applications. To the current knowledge of the authors, there are no studies reporting on the spot welding of dissimilar nanocomposite/unreinforced polymer single lap joints.

In this work, the feasibility of the friction spot welding (FSpW) technique [3] was investigated for single lap joints on poly (methyl methacrylate) (PMMA) 6 N/silica (SiO_2) nanocomposite with a commercial PMMA GS. This new polymer joining technique enables the welding of strong spot joints on similar and dissimilar metallic [4,5] and polymeric materials [6,7] within short welding cycles. The approach of combining a polymeric nanocomposite with tailored properties and a pioneering joining technology offers the possibility of creating lighter component connections with an integration of functions. Thus, various automotive applications would be possible, such as the production of wear-resistant

* Corresponding authors. Address: Helmholtz-Zentrum Geesthacht, Centre for Materials and Coastal Research, Max-Planck-Strasse 1, D-21502 Geesthacht, Germany. Tel./fax: +49 4152 87 2461/2499 (V. Abetz). Tel./fax: +49 4152 87 2066/2033 (S.T. Amancio-Filho).
E-mail addresses: volker.abetz@hzg.de (V. Abetz), sergio.amancio@hzg.de (S.T. Amancio-Filho).
[1] Polymer nanocomposites.
[2] Joining technology.

http://dx.doi.org/10.1016/j.matdes.2014.07.050
0261-3069/

nanocomposite headlamp lenses that can be directly welded to the polymeric housing. This work presents the results on the investigation of the microstructure and material flow in single-lap joints at various rotational speeds. Finally, the mechanical performance of the spot welds with the optimum processing conditions is investigated and compared with other state-of-the-art joining techniques for PMMA.

2. Materials and methods

SiO_2 Ludox HS 40 nanoparticles (Sigma Aldrich Co.) delivered as a monodisperse and colloidal suspension were selected. These nanoparticles have a diameter of 12 nm and a surface area of approximately 220 m^2/g [8]. PMMA Plexiglas® 6 N pellets (Evonik Röhm GmbH, Darmstadt) were used as the matrix material for the nanocomposites. This PMMA grade offers a molecular weight of M_n = 50 kg/mol and an ultimate tensile strength of 67 MPa; a similar ultimate tensile strength of 68 MPa was obtained for the produced PMMA 6 N/2 wt% SiO_2 nanocomposite.

PMMA 6 N/SiO_2 nanocomposites were produced by solution mixing and subsequent extrusion. Round specimens with a diameter of 25 mm and a thickness of 2 mm were produced for microstructural investigations by injection molding. Lap shear testing specimens with dimensions of 100 mm × 25.4 mm × 2 mm according to **ASTM: D1002-10** were compression molded.

Casted PMMA GS plates of 2 mm thickness (Evonik Röhm GmbH, Darmstadt) were machined into specimens with dimensions of 100 mm × 25.4 mm for microstructural and lap shear testing. This PMMA grade exhibits a higher molecular weight M_n = 3065 kg/mol and an ultimate tensile strength of 80 MPa.

Single lap joints were welded on PMMA GS and PMMA/SiO_2 nanocomposite plates using a commercial RPS 100 friction spot welding machine (Harms & Wende, Hamburg, Germany) [9]. Joints were produced with the following parameters: rotational speed of 1000, 2000 and 3000 rpm; a sleeve plunge depth of 2.7 mm (0.7 mm tool penetration in the lower plate), a total joining time of 4.5 s and a clamping force of 2.6 kN.

Microstructural investigations were performed using light optical microscopy (Leica DMIRM) with reflected light. The material flow was analyzed in a Keyence VK-9700 confocal laser microscope. Polarized light microscopy with a Leica DMLM microscope and transmitted light was used to characterize the heat affected zones.

Lap shear testing of the friction spot welds was performed using a Zwick 1478 universal testing machine (Zwick/Roell, Ulm, Germany). The tests were performed at room temperature (23 °C) with a traverse speed of 2 mm min^{-1} according to **ASTM: D1002-10**. Three replicates for the best processing condition were tested.

3. Friction spot welding process

Friction spot welded joints were produced using the "sleeve plunge" technique (Fig. 1). In the process, a titanium TiAl6V4 tool was used, which consisted of a clamping ring, a sleeve and a pin with outer diameters of 14.5, 9 and 6 mm, respectively. Oliveira et al. [6] reported that a titanium tool preserves the generated frictional heat at the spot area due to its low thermal conductivity, resulting in a larger welded volume and thus higher joint strength. First, the PMMA GS plate is placed onto the nanocomposite plate, and the two welding partners are fixed between the clamping ring and the pneumatic piston working as a backing bar (Fig. 1a). The pin and sleeve start to rotate, and the sleeve is plunged into the welding partners; frictional heat is generated in the polymer plates, and the polymer softens. Concomitantly, the pin is retracted (Fig. 1b), creating a cavity. The softened polymer displaced by the plunging action of the sleeve flows into the resulting cavity. By the end of the heating phase, the sleeve retracts while the pin descends, pressing the softened polymer entrapped into the cavity back to the weld, see Fig. 1c. In the last step, the rotation is stopped, and the joint consolidates under pressure to reduce the susceptibility to imperfections due to thermal shrinkage. Finally, the clamping is released, and the welded specimen is removed (Fig. 1d).

4. Results and discussion

Reflective light optical micrographs of the mid-cross section of the spot welds are presented in Fig. 2 for the joints produced using the following process parameters: rotational speeds of 1000, 2000 and 3000 rpm; constant sleeve plunge depth of 2.7 mm; a total joining time of 4.5 s; and a clamping force of 2.6 kN. The spot welds produced with rotational speeds of 1000 rpm and 2000 rpm exhibit similar behavior without any volumetric defects. When welding with a rotational speed of 3000 rpm, excessive heat is generated, inducing softening of the polymer and strong plastic deformation in the spot weld center (i.e., bulging in the lower polymer plate occurs, see white arrow in Fig. 2c). Deformation of the lower plate is an undesired phenomenon and usually reduces the finishing quality of welded parts. At higher temperatures, polymer formability increases because of lower moduli, and the polymeric plate cannot withstand the pressure applied by the tool during the polymer refilling step.

Three different microstructural zones coexist in a thermoplastic friction spot weld [10]. The *stir zone* (SZ) is the area where the sleeve plunges into the polymer plates and where the pin refills the resulting gap with softened polymer. In the SZ, process temperatures above T_g for amorphous and above T_m for semi-crystalline polymers are achieved, and the polymer is locally softened or molten. In this region, significant mixing between the polymers occurs, which can be detected by laser and optical light microscopy as a well-defined zone (Fig. 3a and b). In the *heat affected zones* (HAZ), the temperatures are normally below T_g during the welding process. In these zones, no changes can be visually detected compared with the *base material* (BM).

In a previous study, Oliveira et al. [10] detected a slight decrease in microhardness in this region and were able to determine the extension of this microstructural zone for PMMA spot welds. In

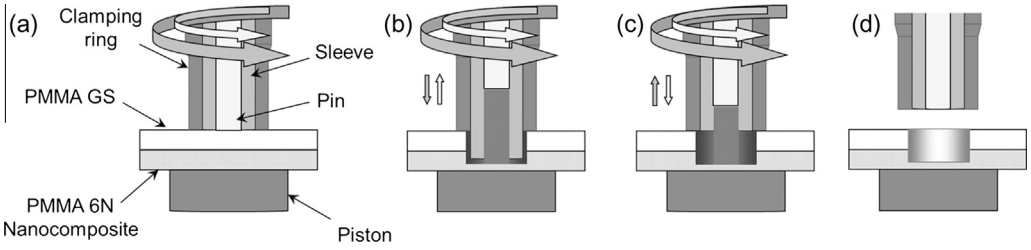

Fig. 1. FSpW process following the "sleeve plunge" technique: (a) clamping of the specimens and onset of pin and sleeve rotation, (b) sleeve is plunged into the polymer plates while the pin is retracted, (c) sleeve is retracted while the pin presses the molten polymer back into the joint, and (d) the tool opens after joint consolidation, and the welded specimen is released.

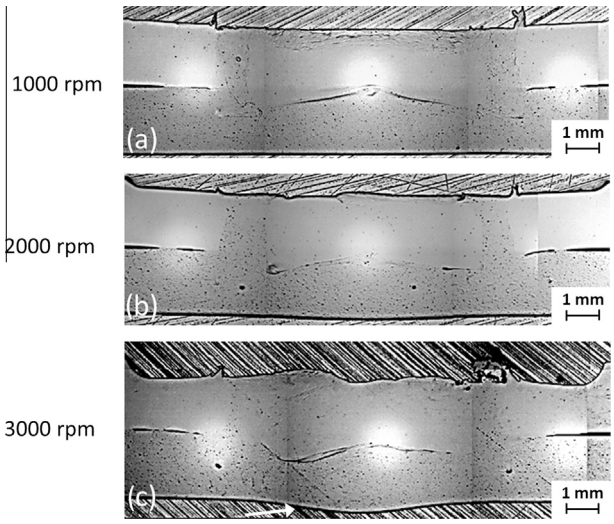

Fig. 2. Optical light microscopy images of PMMA GS/PMMA 6 N-2 wt% SiO_2 joints welded with rotational speeds of (a) 1000 rpm, (b) 2000 rpm and (c) 3000 rpm.

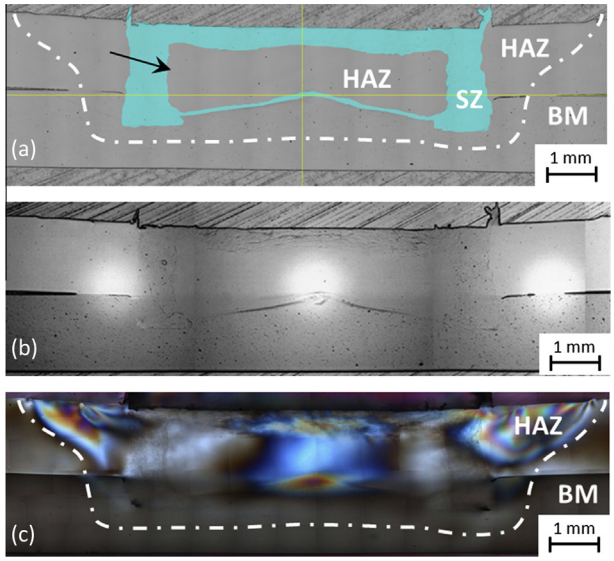

Fig. 3. Example of a PMMA GS/PMMA 6 N-2 wt% SiO_2 joint welded with a rotational speed of 1000 rpm: (a) laser microscopy image with marked SZ, (b) light optical microscopy image and (c) optical polarized light microscopy image with marked outer HAZ. The specimen welded at 1000 rpm was intentionally reproduced from Fig. 2a to facilitate interpretation of the current figure.

the current study, microhardness investigation was unable to identify the extension of the affected zones due to the limitation in size of the produced indentation; no relevant changes in hardness values could be detected in comparison to base material. This may be correlated to the low thermal conductivities of both PMMA GS and the nanocomposites, which contributed to hinder the distribution of frictional heat into the plate, limiting the extent of thermal changes. The exact location of the transition between BM and HAZ could not be determined. Hence the limits of these transitions were only schematically depicted by dash-dot lines in Fig. 3 for illustration purposes. Investigations with nanoindentation testing of smaller volumes within the spot welded volume are in progress to try to evaluate the extension of the HAZ. From the preliminary microstructural investigation (Figs. 2 and 3), the welds produced in this work appear to visually have similar extensions of the stirred zones for the three tested conditions. Further work is required to understand the process-related microstructural changes.

Fig. 3 presents an example of the cross-sectional views of a PMMA GS/PMMA 6 N-2 wt% SiO_2 spot weld. Under reflective optical light microscopy, the different zones of the joint are hardly detectable (Fig. 3b). Transmitted optical microscopy with polarized light was selected in an attempt to provide better contrast for this amorphous polymer. As a result the outer portion of the HAZ could be partially identified and distinguished from the BM (Fig. 3c). Due to the FSpW process, changes in the orientation of the polymer chains occur in this region, resulting in a change in the refraction index of the welded area. In the PMMA/SiO_2 nanocomposite plate, the HAZ cannot be clearly detected because the SiO_2 nanoparticles reflect a large fraction of incident light, and only a small fraction is transmitted.

Thus, a combined use of laser, reflective and transmission polarized optical microscopy was required to detect the presence and extension of the microstructural zones: the SZ and the inner portion of HAZ were detected using laser microscopy (the area indicated by a black arrow, Fig. 3a), while the outer portion of the HAZ (dash-dot line, Fig. 3a) was only partially solved in the upper plate of unreinforced PMMA-GS.

Fig. 4a presents a schematic view of an entire joint with white boxes indicating the areas where the optical light images with higher magnification were recorded. Fig. 4b, d and f show the lower volume of the SZ, and Fig. 4c, e and g show the center of the weld for each welding condition. At a rotational speed of 1000 rpm, a sharp interface (weld line) can be detected in the lower volume of the SZ between the PMMA GS and the PMMA/2 wt% SiO_2 nanocomposite (Fig. 4b). Welding lines are weak links in processed polymeric parts [11] and should be avoided in welded parts. This effect is most likely related to the weld produced at a rotational speed of 10,000 rpm having the lowest heat input of all three tested welding conditions. Lower rotational speeds in friction spot welding have been reported to decrease heat generation [5], resulting in less effective softening and interdiffusion of macromolecules

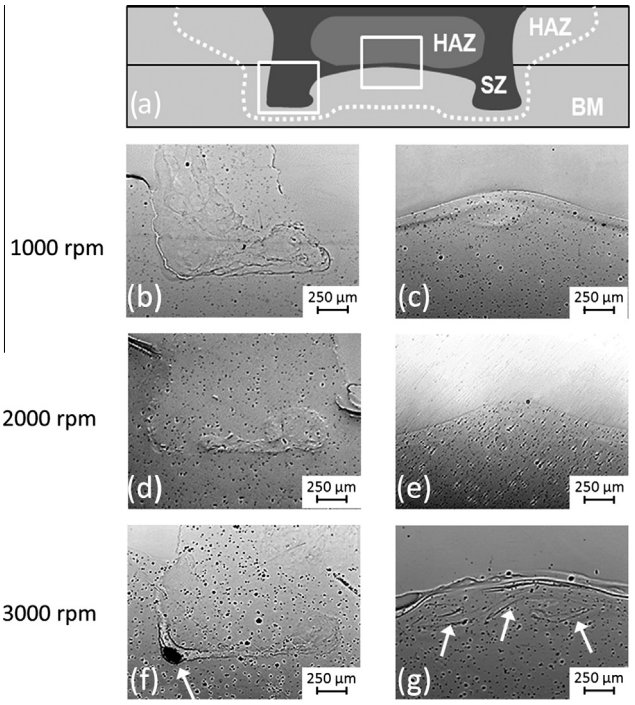

Fig. 4. (a) Schematic view of a PMMA GS/PMMA 6 N-2 wt% SiO_2 spot weld; the white boxes indicate the areas examined at higher magnification. (b, d, f) Magnified light optical micrographs of the lower volume of the SZ and (c, e, g) of the joint center for the investigated welds.

of the polymer plates and the formation of a well-defined weld line. With an increase in the rotational speed to 2000 rpm, polymeric softening was observed (Fig. 4d); higher heat inputs led to improved material mixing and molecular interdiffusion, and the contours of the weld line became smoother.

For the joints welded at a rotational speed of 3000 rpm, no further improvement in material mixing and molecular diffusion could be observed (Fig. 4f). Volumetric defects (see white arrow) were identified in the lower volume of the SZ, which can be explained due to the excess of heat input into the joint and limited material refilling at the spot weld. These flaws were also observed by Oliveira et al. [10] for non-optimized, unreinforced PMMA overlap joints. Volumetric flaws in the friction-based joining of thermoplastics can be associated with several process-related changes [12], including thermal degradation, the evolution of structural or absorbed water and entrapped air related to the tool movement and material mixing. Work is in progress to attempt to understand the source and formation mechanisms of the observed defects.

At a rotational speed of 1000 rpm, a sharp welding line is observed in the center of the weld without any volumetric defects between the polymer plates (Fig. 4c), following the same trend observed for the lower portion of the SZ (Fig. 4b). Following the same trend, the sample welded with the higher heat input of 2000 rpm presents a smoother transition between the polymer plates (Fig. 4e) without volumetric defects along the welding line. According to the polymer welding theory introduced by Wool and O'Connor [13] describing the formation and physics of weld lines, a larger amount of wetting is most likely occurring in the spot weld center between the two polymeric matrices for the joints produced at rotational speeds of 1000 and 2000 rpm, respectively. Complete macromolecular interdiffusion at the overlap interface – a condition for the absence of a weld line – does not occur.

When welding at a rotational speed of 3000 rpm, the joint center contained an inhomogeneous welding line characterized by an entangled interface between the consolidated polymeric material from both the upper and lower plates (see arrows in Fig. 4g). Lin and Wu [14] observed similar results in the spin friction welding of PMMA; at higher heat inputs, obtained using longer frictional times, twisting and entangling in the softened region in the central part of the weld occurred. These authors associated this phenomenon with the formation of a larger softened region near the central part, resulting in twisting and entangling of the softened polymer in this area.

From the microstructural investigation, the rotational speed of 2000 rpm was observed to generate the optimal results in this study, with defect-free welds characterized by a less pronounced weld line and a more homogeneous material mixing at the interface between the upper and lower plates. Therefore, this welding condition was selected for further mechanical characterization using lap shear testing.

The overlap joints of PMMA GS/PMMA 6 N-2 wt% SiO_2 welded at 2000 rpm exhibited average lap shear strength of 3.9 ± 0.05 MPa (Fig. 5a). The final failure occurred by a crack nucleated at the end of the welded area at the plates' interface and finally propagated through the nanocomposite base plate at the interface between the base material and welded area (see Fig. 5b). Although further investigation is required to better understand the failure mechanisms of friction spot welds, one can generally say that the observed type of failure is associated with strong spot welds. The failure in thermoplastic single lap joints was reported by Bilici and Yukler [15] for high density polyethylene friction stir spot welds. The authors observed that the strongest spot welds showed failure modes under lap shear testing similar to the current results. Arici and Mert [16] also observed this behavior in strong polypropylene friction stir spot welds; they reported that the final failure occurred in the base material of one welding partners in a similar manner as reported in this study. Oliveira et al. [10,17] reported identical type of failure for optimized unreinforced PMMA friction spot welds. Generally speaking, when crack path in friction spot single-lap joints of brittle plastics follows the direction of the welded ligament present at the interface between plates, final failure occurs by separation of upper and lower joining partners (the so called "through-the-weld" final failure takes place). This phenomenon indicates that the welded volume is weaker than the base material, usually leading to decreased global mechanical performance of weld.

To the current knowledge of the authors, there is no reference of published work in the field of spot welding of nanocomposites. Therefore, a direct comparison could not be made with the literature. An attempt to evaluate the mechanical performance produced in this study is presented in Fig. 5a. The figure presents the average results of three replicates of the 2000 rpm specimen in a qualitative comparison with the lap shear strengths of unreinforced PMMA welded using state-of-the-art techniques. Compared with the previously published results of friction spot welds on unreinforced PMMA GS 3 mm plates [10] (ultimate shear strength of 9.8 MPa), the PMMA GS/PMMA 6 N-2 wt% SiO_2 spot welds exhibited smaller shear strengths. A possible explanation may be associated with the different plate thicknesses (2 mm for the current welds and 3 mm for the unreinforced PMMA welds) artificially inducing a non-symmetrical stress distribution (i.e., the presence of differential secondary-bending) during the lap shear testing of single lap welds. Thicker single polymeric plates decrease the susceptibility to secondary-bending related stress concentration; in other words, larger plate thicknesses usually result in more uniform shear stress distribution in the spot lap weld and, thus, to

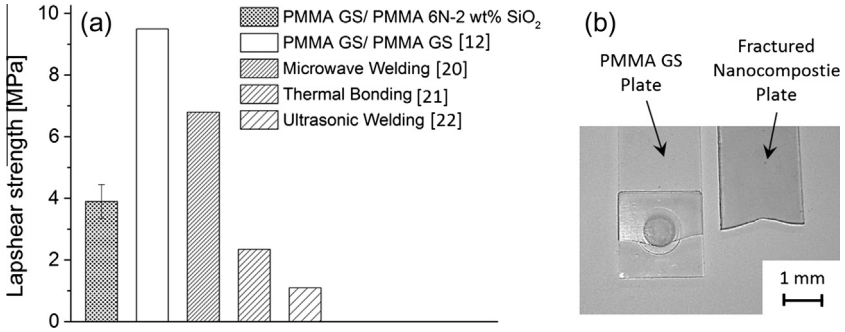

Fig. 5. (a) Lap shear strength of PMMA GS/PMMA 6 N-2 wt% SiO_2 nanocomposite joints welded at a rotational speed of 2000 rpm compared with state-of-the art PMMA welds, (b) fractured PMMA GS/PMMA 6 N-2 wt% SiO_2 nanocomposite lap shear specimens.

higher shear strength [18]. Moreover, the difference in tensile strength of approximately 16% between the PMMA GS (80 MPa) and the PMMA 6 N/2 wt% SiO_2 nanocomposite (67 MPa) has a similar effect. During mechanical testing, the weaker nanocomposite plate is more susceptible to secondary-bending stresses, resulting in an inhomogeneous load distribution and stress concentration; therefore, premature failure may occur in the nanocomposite (see Fig. 5b), reducing the weld strength.

While microwave welded joints exhibited better performance on unreinforced PMMA (maximum value in ultimate lap shear strength of 6.8 MPa [19]), the current results on PMMA 6 N/2 wt% SiO_2 dissimilar welds demonstrated equal or even higher shear strengths when compared with thermal bonded joints [20] with a maximum shear strength of 2.35 MPa and ultrasonic welds [21] with an average lap shear strength of 1.1 MPa. Considering that the work remains in its initial phase and that the optimization phase remains in progress, an improvement of the weld performance can be expected.

5. Conclusions

In the present work, the feasibility of the FSpW of PMMA GS and a PMMA 6 N/2 wt% SiO_2 nanocomposite was successfully demonstrated. The effect of various rotational speeds on the joint microstructure was investigated. Joining conditions with a rotational speed of 2000 rpm resulted in a defect-free joint microstructure with a smooth weld line, while single-lap joints produced with reduced (1000 rpm) and excessive (3000 rpm) heat inputs led to volumetric defects and the presence of weld lines. In terms of the mechanical performance, the single overlap joints produced at 2000 rpm achieved a shear strength of 3.9 ± 0.05 MPa, which is comparable to the majority of values observed for PMMA welds produced using state-of-the-art techniques but smaller than that observed with similar PMMA friction spot and microwave welds. This preliminary work indicates the potential of friction spot welding as an alternative technique to produce overlap joints with thermoplastic nanocomposites.

Acknowledgments

We would like to thank Pedro Oliveira for his support with the FSpW. In addition, we would like to thank Heinrich Böttcher and Dr. Prokopios Georgopanos for the tensile testing and Maren Brinkmann for the GPC measurements. Finally, we would like to acknowledge the financial support of the Landesexzellenzcluster "Integrated Material Systems" and the Helmholtz Association through the Young Investigator Group, "Advanced Polymer Metal Hybrid Structures" (Amancio-Filho, Grant No. VH-NG-626).

References

[1] Chakkalakal GL, Alexandre M, Boschetti-de-Fierro A, Abetz V. Effect of silica-coated poly(butyl methacrylate)-block-poly(methyl methacrylate) double-shell particles on the mechanical properties of PMMA composites. Macromol Mater Eng 2012;297:887–93.
[2] Haase A, Hesse P, Brommer L, Jacobs O, Abetz C, Handge UA, et al. Modification of polycarbonate and glycol modified poly(ethylene terephthalate) by addition of silica-nanoparticles grafted with SAN copolymer using "Classical" and ARGET ATRP. Macromol Mater Eng 2013;298:292–302.
[3] Schilling C, dos Santos JF. Method and device for linking at least two adjoining work pieces by friction welding. International Patent Publication; 2005, WO/2001/036144.
[4] Tier MD, Rosendo TS, dos Santos JF, Huber N, Mazzaferro JA, Mazzaferro CP, et al. The influence of refill FSSW parameters on the microstructure and shear strength of 5042 aluminium welds. J Mater Process Technol 2013;213:997–1005.
[5] Amancio Filho ST, Camillo APC, Bergmann L, dos Santos JF, Kury SE, Machado NGA. Preliminary investigation of the microstructure and mechanical behaviour of 2024 aluminium alloy friction spot welds. Mater Trans 2011;52(5):985–91.
[6] Oliveira PHF, Amancio Filho ST, dos Santos JF, Hage Jr. E. Influence of the tool material on the microstructure and mechanical properties of PMMA lap joints welded by friction spot. In: Proc.: ANTEC 2011 PENG, Boston, MA, USA; May, 2011.
[7] Gonçalves J, Amancio Filho ST, dos Santos JF, Canto LB. Friction spot welding (FSpW) of Polyamide 6 and Polyamide 6.6/Carbon Fiber Laminates: Process Improvement by Optimization of Process Parameters and Tool Size. In: Proc.: XXXVIII CONSOLDA – Congresso Nacional de Soldagem, Ouro Preto, MG, Brasil; October, 2012.
[8] LUDOX HS-40 – product information, Grace Davison, <http://doc.ccc-group.com/spec/553701.pdf>, accessed on 6 December 2013.
[9] Reibpunktschweißen, das neue Verfahren – Zwei Ringe, die Zusammenschweißen; product information, Harms & Wende GmbH, <http://85.214.241.35/hwh/files/content/rps100_prospekt_09_161009.pdf>, [accessed 2.10.13].
[10] Oliveira PHF, Amancio-Filho ST, dos Santos JF, Hage Jr E. Preliminary study on the feasibility of friction spot welding in PMMA. Mater Lett 2010;64:2098–101.
[11] Hagerman EM. Weld-Line fracture in molded parts. Plast Eng 1973;29:67.
[12] Amancio-Filho ST, Roeder J, Nunes SP, dos Santos JF, Beckmann F. Thermal degradation of polyetherimide joined by friction riveting (FricRiveting). Part I: influence of rotation speed. Polym Degradation Stability 2008;93:1529–38.
[13] Wool RP, O'Connor KM. A theory of crack healing in polymers. J Appl Phys 1981;52:5953–63.
[14] Lin CB, Wu LC. Friction welding of similar and dissimilar materials: PMMA and PVC. Polym Eng Sci 2000;40:1931–41.
[15] Bilici MK, Yukler AI. Effects of welding parameters on friction stir spot welding of high density polyethylene sheets. Mater Des 2012;33:545–50.
[16] Arici A, Mert S. Friction stir spot welding of polypropylene. J Reinforced Plast Compos 2008;27(18):2001–4.
[17] Oliveira PHF. Estudo das propriedades e desempenho mecânico de juntas soldadas por fricção pontual de poli (metacrilato de metila) (PMMA), MSc thesis, Universidade Federal de São Carlos, 2012.
[18] Schürmann H. Konstruieren mit Faser-Kunststoff-Verbunden. 2. Auflage. Germany, Heidelberg: Springer-Verlag; 2007.
[19] Yussuf AA, Sbarski I, Hayes JP, Tran N, Solomon M. Rapid microwave welding of two polymethylmethacrylates substrates. ANTEC 2004:1256–60.
[20] Sood V. An experimental study on thermal bonding effects of PMMA based microdevices using hot embossing, MSc thesis, University of Texas, Arlington; 2007.
[21] Souza JM. Study and mechanical evaluation of ultrasonic joints of polycarbonate and poly(methyl methacrylate), MSc thesis, São Paulo: Polytechnic School of University of São Paulo; 2005.